

Particle Diameter Effect on Heat Transfer Due to Natural Convection Using Cu-Water Nanofluid – A Non-Newtonian Approach

Apurba Kumar Santra^a, Swarnendu Sen^b, Niladri Chakraborty^c

^aDepartment of Power Engineering, Jadavpur University, Salt Lake Campus, Block – LB, Plot-8, Sector – III, Salt Lake, Kolkata – 700 098, India. e-mail: aksantra@pe.jusl.ac.in

^bDepartment of Mechanical Engineering, Jadavpur University, Kolkata- 700 032, India. e-mail: drssen@mech.jdvu.ac.in

^cDepartment of Power Engineering, Jadavpur University, Salt Lake Campus, Block – LB, Plot-8, Sector – III, Salt Lake, Kolkata – 700 098, India. e-mail:chakraborty_niladri2004@yahoo.com

ABSTRACT

Heat transfer due to laminar natural convection in a differentially heated square cavity using copper-water nanofluid has been studied numerically. The nanofluid is Non-Newtonian. The shear stresses have been calculated using Ostwald-de Waele model (power law model). The transport equations for a non-Newtonian fluid have been discretised using finite volume approach and solved following SIMPLER algorithm through ADI method. The thermal conductivity of the nanofluid has been calculated from the model proposed by Patel *et al.* Study has been conducted for Rayleigh number (Ra) varying from 10^4 to 10^7 while solid volume fraction (ϕ) of copper particles in water have been varied from 0.05% to 5%. Study has been conducted for different particle size of copper ranging from 50 nm to 100 nm. The general trend is that for a particular Rayleigh number and particular solid volume fraction of the nanoparticles, the heat transfer increases with decreases in particle size at higher Ra . For lower Ra the heat transfer first decreases and then increases.

Nomenclature

c	specific heat (J/kg K)
Gr_f	Grashof number of fluid, $\rho^2 g \beta \Delta T H^3 / \mu^2$
g	acceleration due to gravity (m/s^2)
h, l	dimensional (m) height and width of cavity
k	thermal conductivity (W/mK)
m, n	the respective consistency and fluid behaviour index parameters,
Nu_y	local Nusselt number of the heater
\overline{Nu}	average Nusselt number at the heater
P	pressure (N/m^2)
p	dimensionless pressure $(p-p_0)H^2/\rho_0\alpha^2$
Pr	Prandtl number of fluid, ν_f/α_f
Ra	Rayleigh Number, $Gr Pr$
T	temperature (K)
T_H, T_C	temperature (K) of the heat source and sink respectively
u, v	velocity components in the x and y directions respectively (m/s)
U, V	dimensionless velocities ($U = uH/\alpha, V = vH/\alpha$)
x, y	horizontal and vertical coordinates respectively (m)
X, Y	dimensionless horizontal and vertical coordinates respectively ($X = x/h, Y = y/h$)

Greek Symbols

α	thermal diffusivity of the fluid (m^2/s)
β	isobaric expansion coefficient (K^{-1})

ϕ	solid volume fraction
μ	dynamic viscosity (N.s/m ²)
ν	kinematic viscosity (m ² /s)
ρ	density of the fluid (kg/m ³)
θ	dimensionless temperature $(T-T_0)/(T_H-T_C)$
ψ	dimensionless stream function
τ	the stress tensor,

Subscripts

eff	effective
f	fluid
nf	nanofluid
0	at reference state
s	solid

1. INTRODUCTION

It has been observed by many researchers that Nanofluid (1–100 nm sized solid particles dispersed in fluid) improves thermal conductivity considerably compared to the base fluid [1, 2, 3]. Xuan *et al.* [3] experimentally obtained thermal conductivity of copper-water nanofluid up to 7.5% of solid volume fraction (ϕ) with 100 nm diameter copper particles, which remains stable for more than 30 hours without disturbance. These nanofluids are stable [4], introducing very little pressure drop and can pass through micro-channels. Stabilizers like oleic acid and laurate salt also can be added [5]. Several views regarding mechanism of heat transfer enhancement is available [6, 7] of which thermal dispersion, Brownian motion of the particles, molecular level layering of liquid at the liquid/particle interface, ballistic phonon transport through the particles and nanoparticle clustering are important. Das *et al.* [8] have shown that effective thermal conductivity (k_{eff}) of nanofluid increases with increase in temperature. So it can sense the high heat flux zones.

Several models have been proposed to determine the k_{eff} of nanofluid. The models, proposed by Hamilton & Crosser (HC) [9], Wasp [10], Maxwell-Garnett [11] and Bruggeman [12], show the effect of thermal conductivity of clear fluid & solid and the solid volume fraction on k_{eff} . But all these models fail to predict the thermal conductivity enhancement accurately [2] as experimental results showed much higher thermal conductivity.

Chon *et al.* [13] have shown experimentally that k_{eff} increases with increase in temperature as well as ϕ and with the decrease in particle diameter (d_p). Patel *et al.* [14] have proposed a model, applicable for low concentration of nanoparticles, which is a function of temperature and particle size. There involves an empirical constant 'c', which can be found by comparing the calculated value with experimental data [14].

Khanafer *et al.* [15] have performed a numerical study of heat transfer enhancement following Wasp model [10] using copper nanofluid in a differentially heated square cavity. They have considered the thermal dispersion but that involves an empirical constant, which is still unknown. Jou *et al.* [16] have performed same study as of [15] to observe the effect of aspect ratio of the enclosure on heat transfer for Cu-water nanofluid considering ϕ upto 20%.

Putra *et al.* [17] and Wen and Ding [18] have carried out experiments with natural convection. They have shown that heat transfer decreases with increase in solid volume fraction. This may be due to non-Newtonian character of nanofluid at low shear rate. Nnanna [19] have experimentally observed for differentially heated square cavity that the Nusselt number strongly depends on the amount of solid volume fraction even for a lower range of Rayleigh number. He has observed increase in heat transfer for lower solid volume fraction ($2.0\% \geq \phi \geq 0.2\%$). However beyond $\phi = 2\%$ the heat transfer decreases due to increase in kinematic viscosity of the nanofluid.

Kwak and Kim [20], Chang *et al.* [21], Ding *et al.* [22] have shown experimentally that nanofluid have non-Newtonian character and shear thinning in nature. Recently Santra *et al.* [23] have numerically investigated the heat transfer in a differentially heated square cavity considering non-Newtonian power law model for copper-water nanofluid. Their findings are similar to that of Ref. 17 and 18.

Very few research papers have been found to observe the effect of particle diameter on heat transfer characteristics of nanofluid. Lee *et al.* [1] and Xuan and Li [3] have used particles of approximately

100 nm diameter. Eastman *et al.* [2] had used copper particles of less than 10 nm diameter, which was prepared by one step method. Chon *et al.* [13] had used alumina particles of three different sizes i.e., 11 nm, 47 nm and 150 nm nominal diameter while Patel *et al.* had used alumina particle of 11 nm diameter [14] and gold particles of 10–20 nm diameter for their study [5]. Putra *et al.* [17] have studied with 131.2 nm and 87.3 nm sized particles for Al₂O₃ and CuO respectively. Wen and Ding [18] had used TiO₂ particles of about 34 nm average diameter while Nnanna [19] had used Al₂O₃ particles of 27 nm diameter. Thus it is observed that different researchers have used different type of nanofluid with a variety of particle sizes for their study.

So far as no systematic study has been performed to observe the effect of particle size on the heat transfer (except some experiment in Ref.13). The present paper shows the size-effect of nanoparticles on the heat transfer due to natural convection in a differentially heated square cavity considering the nanofluid as non-Newtonian. To determine the effective thermal conductivity (k_{eff}) of the nanofluid, model given by Patel *et al.* [14] has been used with appropriate value of ‘c’, which has been calculated by matching with the experimental results [3]. The viscosity of nanofluid has been calculated using Ostwald-de Waele model (two parameter power law model) for a non-Newtonian shear thinning fluid [23]. Here the authors have used the primitive variables.

2. MATHEMATICAL FORMULATION

2.1. Problem Statement

Figure 1 shows the geometry of the present problem. It is a two-dimensional square enclosure of height h and width l . The temperatures of the two sidewalls of the cavity are maintained at T_H and T_C , where T_C has been considered as the reference condition. The top and the bottom horizontal walls have been considered to be insulated. The enclosure is filled with a mixture of water and solid spherical copper particles of 100 nm diameter. The nanoparticles are of uniform shape and size. The nanofluid is assumed to be non-Newtonian, incompressible and the flow is laminar. Also it is assumed that the liquid and solid are in thermal equilibrium and they flow at same velocity. The density varies only in buoyant force, which has been incorporated only in the body force term by employing the Boussinesq approximation. For all the studies $h = l$ has been considered.

2.2. Governing Equations and Boundary Conditions

The continuity, momentum and energy equations for a steady, two-dimensional flow of copper-water nanofluid has been considered. The Fluid follows the Fourier Law of heat conduction and its property do not change with temperature. The non-dimensional governing equations for a steady, two-dimensional flow are as follows

$$\frac{\partial u}{\partial x} + \frac{\partial v}{\partial y} = 0., \tag{1}$$

$$\rho_{nf,o} \left(u \frac{\partial u}{\partial x} + v \frac{\partial u}{\partial y} \right) = - \frac{\partial p}{\partial x} - \left[\frac{\partial \tau_{xx}}{\partial x} + \frac{\partial \tau_{yx}}{\partial y} \right] \tag{2}$$

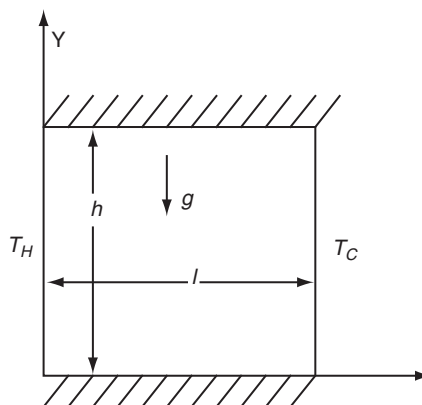


Figure 1. Geometry of the present problem.

$$\rho_{nf,0} \left(u \frac{\partial v}{\partial x} + v \frac{\partial v}{\partial y} \right) = -\frac{\partial p}{\partial y} + [\phi \rho_{s,0} \beta_s + (1-\phi) \rho_{f,0} \beta_f] g(T - T_C) - \left[\frac{\partial \tau_{xy}}{\partial x} + \frac{\partial \tau_{yy}}{\partial y} \right] \quad (3)$$

$$u \frac{\partial T}{\partial x} + v \frac{\partial T}{\partial y} = \alpha_{nf} \left[\frac{\partial^2 T}{\partial x^2} + \frac{\partial^2 T}{\partial y^2} \right] \quad (4)$$

where,

$$\alpha_{nf} = \frac{k_{nf}}{(\rho C p)_{nf,0}} \quad (5)$$

where the relationships between the shear stress and shear rate in case of two-dimensional motion in rectangular co-ordinate according to the Ostwald-de Waele model are as follows: [24]

$$\tau = -m \left[\left| \sqrt{\frac{1}{2} (\dot{\gamma} \cdot \dot{\gamma})} \right|^{(n-1)} \right] \dot{\gamma} \quad (6)$$

where

$$\frac{1}{2} (\dot{\gamma} \cdot \dot{\gamma}) = 2 \left\{ \left(\frac{\partial u}{\partial x} \right)^2 + \left(\frac{\partial v}{\partial y} \right)^2 \right\} + \left(\frac{\partial v}{\partial x} + \frac{\partial u}{\partial y} \right)^2 \quad (7)$$

Thus the stress tensors of the equations (2) and (3) take the following forms

$$\tau_{xx} = -2 \left\{ m \left[\left| 2 \left\{ \left(\frac{\partial u}{\partial x} \right)^2 + \left(\frac{\partial v}{\partial y} \right)^2 \right\} + \left(\frac{\partial v}{\partial x} + \frac{\partial u}{\partial y} \right)^2 \right|^{\frac{1}{2}} \right|^{(n-1)} \right] \left(\frac{\partial u}{\partial x} \right) \right\} \quad (8)$$

$$\tau_{yx} = \tau_{xy} = - \left\{ m \left[\left| 2 \left\{ \left(\frac{\partial u}{\partial x} \right)^2 + \left(\frac{\partial v}{\partial y} \right)^2 \right\} + \left(\frac{\partial v}{\partial x} + \frac{\partial u}{\partial y} \right)^2 \right|^{\frac{1}{2}} \right|^{(n-1)} \right] \left(\frac{\partial u}{\partial y} + \frac{\partial v}{\partial x} \right) \right\} \quad (9)$$

$$\tau_{yy} = -2 \left\{ m \left[\left| 2 \left\{ \left(\frac{\partial u}{\partial x} \right)^2 + \left(\frac{\partial v}{\partial y} \right)^2 \right\} + \left(\frac{\partial v}{\partial x} + \frac{\partial u}{\partial y} \right)^2 \right|^{\frac{1}{2}} \right|^{(n-1)} \right] \left(\frac{\partial v}{\partial y} \right) \right\} \quad (10)$$

Here m and n are two empirical constants, which depends on the type of nanofluid used. For the present case the values of 'm' and 'n' has been taken from published results. Detail of the values of m and n can be obtained from Ref. 23.

The effective density of the nanofluid at reference temperature is

$$\rho_{nf,0} = (1-\phi) \rho_{f,0} + \phi \rho_{s,0} \quad (11)$$

and the heat capacitance of nanofluid is

$$(\rho C p)_{nf} = (1-\phi) (\rho C p)_f + \phi (\rho C p)_s \quad (12)$$

as given by Xuan *et al.* [6].

The effective thermal conductivity of the nanofluid has been determined by the model proposed by Patel *et al.* [14]. For the two-component entity of spherical-particle suspension the model gives

$$\frac{k_{eff}}{k_f} = 1 + \frac{k_p A_p}{k_f A_f} + c k_p Pe \frac{A_p}{k_f A_f} \quad (13)$$

where
$$\frac{A_p}{A_f} = \frac{d_f}{d_p} \frac{\phi}{(1-\phi)} \tag{14}$$

and $Pe = \frac{u_p d_p}{\alpha_f}$, where u_p is the Brownian motion velocity of the particles which is given by

$$u_p = \frac{2k_b T}{\pi \mu_f d_p^2}.$$

The calculation of effective thermal conductivity can be obtained from equation (13).

The above equations can be converted to non-dimensional form, using the following dimensionless parameters $X = x/h$, $Y = y/h$, $U = uh/\alpha$, $V = vh/\alpha$, $P = (p - p_0) \cdot h^2/(\rho_{nf,0} \cdot \alpha^2)$ and $\theta = (T - T_C)/(T_H - T_C)$ Then

The non-dimensional equations will be as follows

$$\frac{\partial U}{\partial X} + \frac{\partial V}{\partial Y} = 0 \tag{15}$$

$$U \frac{\partial U}{\partial X} + V \frac{\partial U}{\partial Y} = -\frac{\partial P}{\partial X} + \frac{\mu_{app}}{\rho_{nf,0} \alpha_{f,0}} \left[\frac{\partial^2 U}{\partial X^2} + \frac{\partial^2 U}{\partial Y^2} \right] \tag{16}$$

$$U \frac{\partial V}{\partial X} + V \frac{\partial V}{\partial Y} = -\frac{\partial P}{\partial Y} + Gr Pr Pr \frac{\rho_{f,0}}{\rho_{nf,0}} (1-\phi + \phi \frac{\rho_s \beta_s}{\rho_f \beta_f}) \theta + \frac{\mu_{app}}{\rho_{nf,0} \alpha_{f,0}} \left[\frac{\partial^2 V}{\partial X^2} + \frac{\partial^2 V}{\partial Y^2} \right] \tag{17}$$

$$U \frac{\partial \theta}{\partial X} + V \frac{\partial \theta}{\partial Y} = \frac{k_{nf}}{k_f} \frac{(\rho C p)_{f,0}}{(\rho C p)_{nf,0}} \left[\frac{\partial^2 \theta}{\partial X^2} + \frac{\partial^2 \theta}{\partial Y^2} \right] \tag{18}$$

Here the apparent viscosity of the nanofluid is

$$\mu_{app} = m \left(\frac{\alpha_{f,0}}{h^2} \right)^{(n-1)} \left[2 \left\{ \left(\frac{\partial U}{\partial X} \right)^2 + \left(\frac{\partial V}{\partial Y} \right)^2 \right\} + \left(\frac{\partial V}{\partial X} + \frac{\partial U}{\partial Y} \right)^2 \right]^{\frac{1}{2}} \tag{19}$$

The boundary conditions, used to solve equations (15) to (18) are as follows.

$$U = V = \frac{\partial \theta}{\partial Y} = 0 \text{ at } Y = 0, 1.0 \text{ and } 0 \leq X \leq 1.0.$$

$$\theta = 1.0 \text{ and } U = V = 0 \text{ at } X = 0 \text{ and } 0 \leq Y \leq 1.0.$$

$$\theta = 0 \text{ and } U = V = 0 \text{ at } X = 1.0 \text{ and } 0 \leq Y \leq 1.0.$$

Equations. (15) to (18), along with the boundary conditions are solved numerically. From the converged solutions, values of Nu_y (Local Nusselt number) and \overline{Nu} (Average Nusselt number) for the hot wall has been calculated.

$$Nu_y = -\frac{k_{eff}}{k_f} \frac{\partial \theta}{\partial X} \Big|_{x=0,y} \tag{20}$$

$$\overline{Nu} = \frac{1}{H} \int_0^H Nu_y \cdot dY \Big|_{x=0} \tag{21}$$

where, H is dimensionless cavity height.

The dimensionless stream function ψ has been defined as $U = \partial\psi/\partial Y$ and $V = -\partial\psi/\partial X$. The stream function at any grid location (X, Y) is calculated as

$$\psi(X, Y) = \int_{Y_0}^Y U \cdot \partial Y + \psi(X, Y_0) \tag{22}$$

Along the solid boundary the stream function is taken as zero. $\psi(X, Y_0)$ is known either from the previous calculation, or, from the boundary condition.

3. NUMERICAL APPROACH AND VALIDATION

The governing mass, momentum and energy equations has been discretised by a control volume approach using a power law profile approximation. The computational domain has been divided into 81×81 non-uniform grids. Finer grids have been taken at the boundaries. Before selecting the number of grids, a grid independence study has been conducted. Average Nusselt numbers for particle diameter of 50 nm, for $Ra = 10^7$ and $\phi = 5\%$ for different number of grids has been summarized in Table 1. It has been found that the variation in average Nusselt number among grids 81×81 and 91×91 is less than 0.02%.

Table 1: Result of grid independence study (for $d_p = 50$ nm and $Ra = 10^7$ with $\phi = 5\%$)

Number of grids	Average Nusselt number	% change in Average Nusselt number
61 by 61	37.017044	
71 by 71	37.030992	0.037679868
81 by 81	37.040475	0.025609119
91 by 91	37.047618	0.019284168

The set of discretized equations have been solved iteratively, through alternate direction implicit ADI, using the SIMPLER algorithm [25]. For convergence, under-relaxation technique has been employed. To check the convergence, the mass residue of each control volume has been calculated and the maximum value has been used to check the convergence. The convergence criterion has been set to 10^{-7} .

The results of present code closely matches with de Vahl Davis [26] for different Ra . In that case air has been considered as working fluid, which is Newtonian in nature (i.e. $n = 1$). It has been found that for Rayleigh no. (Ra) 10^3 , 10^4 , 10^5 and 10^6 the values of \overline{Nu} are 1.118, 2.245, 4.521 and 8.813 respectively for our case while 1.118, 2.243, 4.519 and 8.799 respectively for de Vahl Davis.

4. RESULTS AND DISCUSSIONS

The study has been conducted for $d_p = 50$ nm to 100 nm with an increment of 10 nm, $Ra = 10^4$ to 10^7 , and ϕ for 0% to 5% with increment of 0.5%. Prandtl no. of base fluid (water) is 7.02. The thermo-physical properties of both the solid and the fluid have been summarized in Table 2.

The effective thermal conductivity of nanofluid has been calculated using the correlation given in [14] for each control volume as the k_{eff} is temperature dependent. The constant 'c' which appears in the correlation has been calculated from the experimental data available for copper water nanofluid [3]. The average value of constant has been considered for our simulation, which came out as 3.60×10^4 that is in line with result given in Ref.14. The hot wall temperature has been considered as 303 K (30°C) while the cold wall temperature is 293 K (20°C). The shear stresses have been calculated using Ostwald-de Waele model for an incompressible non-Newtonian fluid. The constants m and n for calculating shear stresses have been taken from the experimental observation [17].

4.1. Effect of Particle Size on Vertical Velocity and Temperature

The vertical velocities for different particle diameter at $Y = 0.5$ for $1.0 \geq X \geq 0.0$, for $\phi = 2.5$ $Ra = 10^6$ has been presented in Figure 2, which shows that with the increase in d_p , the value of maximum velocity decreases. This is caused by decrease in specific surface area (i.e surface area of the particles

Table 2: Thermo-physical properties of different phase at 20°C

Property	Fluid (water)	Solid (copper)
C_p (J/Kg K)	4181.80	383.1
ρ (Kg/m ³)	1000.52	8954.0
k (W/m K)	0.597	386.0
β (K ⁻¹)	210.0×10^{-6}	51.0×10^{-6}

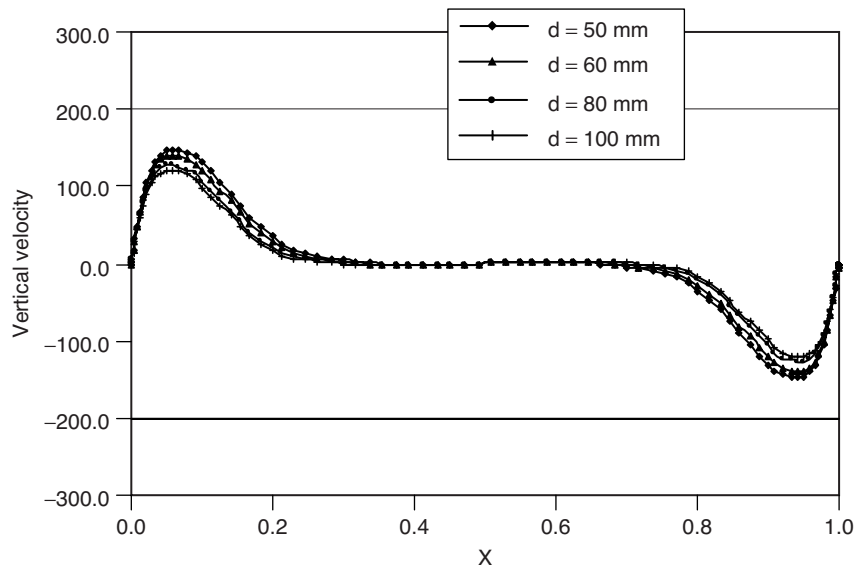


Figure 2. Vertical velocity at mid plane for $\phi = 2.5$ $Ra = 10^6$ for various particle diameter.

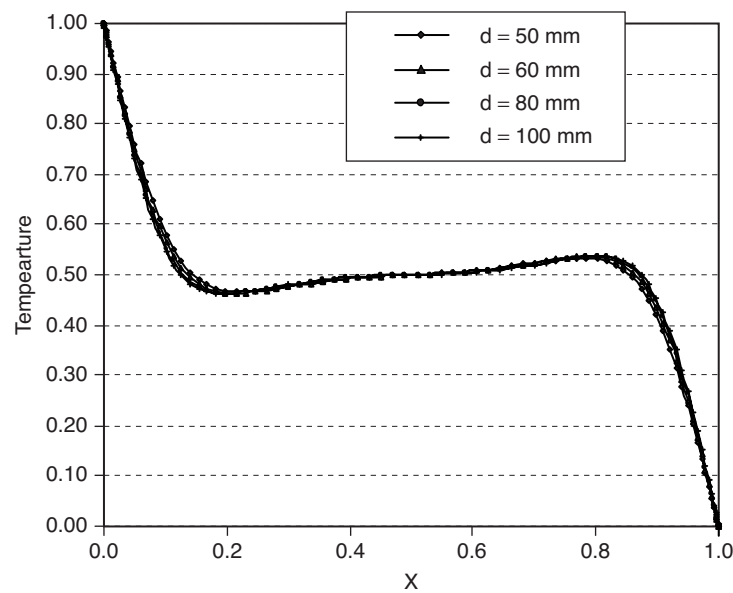


Figure 3. Temperature at mid plane for $\phi = 2.5$ $Ra = 10^6$ for various particle diameter.

per unit mass of copper) of the particles, with increase in d_p which in turn decreases the convective heat transfer. Hence buoyancy decreases and heat transfer decreases. This feature is true for other Rayleigh numbers also.

Figure 3 shows the variation of temperature along the mid-plane of the cavity for $Ra = 10^6$ and $\phi = 2.5\%$. This shows that a uniform temperature prevails at the core of cavity because there is no flow. With the decrease in d_p , this zone increases slightly. This feature is true for other Rayleigh numbers also.

4.2. Effect of Particle Size and Solid Volume Fraction on Average Nusselt Number

The average Nusselt number (\overline{Nu}) along the hot wall has been presented for different particle diameter and ϕ for $Ra = 10^6$ in Figure 4. It shows a steady decrease in \overline{Nu} for increase in ϕ for same Ra when particle size exceeds 70 nm. The trend is similar to that observed from the experiments of Putra *et al.* [17] and Wen and Ding [18]. Also \overline{Nu} increases with decrease in d_p for a particular ϕ . This observation is true for other Ra also.

Particle Diameter Effect on Heat Transfer Due to Natural Convection Using Cu-Water Nanofluid – A Non-Newtonian Approach

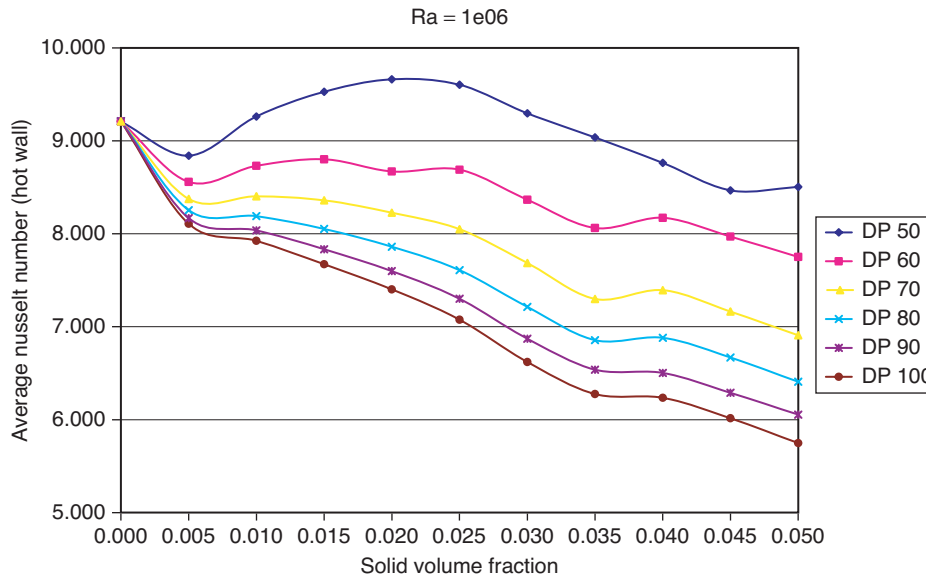


Figure 4. Average Nusselt Number of LHS wall for $Ra = 10^6$ for various particle diameter and ϕ .

This is because at higher particle size the viscosity of nanofluid increases with increase in ϕ . Hence convective heat transfer decreases, which in turn decreases the average Nusselt number. But as the particle size is lowered, heat transfer increases at lower ϕ i.e. upto 2% because of increase in convective heat transfer as effective thermal conductivity of nanofluid increases with ϕ . The effective thermal conductivity of the nanofluid increases with decrease in d_p , because of increase in specific surface area (or surface to volume ratio) of nanoparticles. Beyond 2% it decreases again as increase in viscosity dominates over increase in thermal conductivity.

For $Ra = 10^7$ the same trend can be observed only the point of maximum Nusselt number shifts to $\phi = 2.5\%$. Similarly for $Ra = 10^5$ the same trend can be observed only the point of maximum Nusselt number shifts to the left i.e., $\phi = 1.5\%$. Also it is observed that for $d_p = 50$ the value of maximum Nusselt number decreases with decrease in Ra .

It is very interesting to note that as particle size increases the heat transfer decreases rapidly (Figure 5).

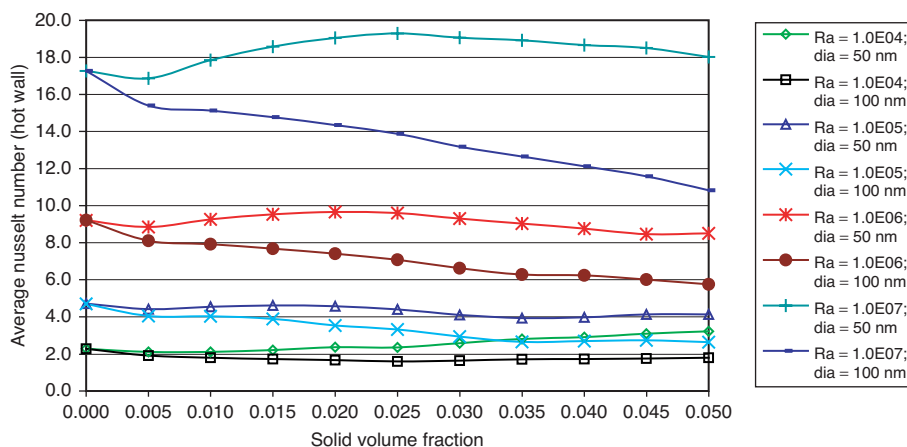


Figure 5. Variation of Average Nusselt Number of LHS wall with Ra and ϕ , for $d_p = 50$ and 100.

5. CONCLUSIONS

Heat transfer due to laminar natural convection in a differentially heated square cavity using copper-water nanofluid has been studied numerically. Study has been conducted for different copper particle size (50 nm to 100 nm) for different Ra (10^4 to 10^7) and (0.05% to 5%).

It has been observed that with decrease in particle size, vertical velocity at the mid-plane increases for a particular Rayleigh number and particle size. A large no flow core zone is observed. While the temperature distribution shows a large isothermal core which almost remain intact with change in particle size. Heat transfer increases with decrease in particle size for a particular amount of solid for any Ra . For higher particle size (70 nm and above) heat transfer gradually decreases. For particle size 50 nm and 60 nm the heat transfer first increases and then decreases. This point of maximum heat transfer also depends on the value of Rayleigh number and solid volume fraction.

Detail experiments need to be carried out to observe the actual behaviour of nanofluid with different particle size.

REFERENCES

- [1] Lee, S., Choi, S.U.S., Li, S. and Eastman, J.A., Measuring Thermal Conductivity of Fluids Containing Oxide Nanoparticles, *ASME J. of Heat Transfer*, 1999, 121 (2), 280-289.
- [2] Eastman, J.A., Choi, S.U.S., Li, S., Yu, W. and Thompson, L.J., Anomalous Increased Effective Thermal Conductivities of Ethylene Glycol-Based Nanofluids Containing Copper Nanoparticles, *Applied Physics Letters*, 2001, 78 (6), 718-720.
- [3] Xuan, Y. and Li, Q., Heat Transfer Enhancement of Nanofluids, *Int. J. Heat and Fluid Flow*, 2000, 21 (1), 58-64.
- [4] Zhou, D.W., Heat Transfer Enhancement of Copper Nanofluid with Acoustic Cavitation, *Int. J. Heat and Mass Transfer*, 2004, 47 (14-16), 3109-3117.
- [5] Patel, H.E., Das, S.K., Sundararajan, T., Nair, A.S., George, B. and Pradeep, T., Thermal conductivities of naked and monolayer protected metal nanoparticle based nanofluids: Manifestation of anomalous enhancement and chemical effects, *Applied Physics Letters*, 2003, 83(14), 2931-2933.
- [6] Xuan, Y. and Roetzel, W., Conceptions for Heat Transfer Correlation of Nanofluids, *Int. J. Heat and Mass Transfer*, 2000, 43 (19), 3701-3707.
- [7] Keblinski, P., Phillpot, S.R., Choi, S.U.S. and Eastman, J.A., Mechanisms of Heat Flow in Suspensions of Nano-sized Particles (Nanofluids), *Int. J. Heat and Mass Transfer*, 2002, 45 (4), 855-863.
- [8] Das, S.K., Putra, N., Thiesen, P., and Roetzel, W., Temperature Dependence of Thermal Conductivity Enhancement for Nanofluids, *ASME J. of Heat Transfer*, 2003, 125 (4), 567-574.
- [9] Hamilton, R.L. and Crosser, O.K., Thermal conductivity of heterogeneous two-component systems. *I & EC Fundamentals* 1, 1962, 182-191.
- [10] Wasp, F. J., Solid-Liquid Flow Slurry Pipeline Transportation, *Trans. Tech. Pub.*, Berlin, 1977.
- [11] Maxwell-Garnett, J.C., Colours in metal glasses and in metallic films, *Philos. Trans. Roy. Soc. A*, 1904, 203, 385-420.
- [12] Bruggeman, D.A.G., Berechnung Verschiedener Physikalischer Konstanten von Heterogenen Substanzen, I. Dielektrizitätskonstanten und Leitfähigkeiten der Mischkörper aus Isotropen Substanzen. *Annalen der Physik*. Leipzig, 1935, 24, 636-679.
- [13] Chon, H.C., Kihm, K.D., Lee, S.P. and Choi, S.U.S., Empirical correlation finding the role of temperature and particle size for nanofluid (Al₂O₃) thermal conductivity enhancement, *Applied Physics Letters*, 2005, 87, 153107.
- [14] Patel, H.E., Sundararajan, T., Pradeep, T., Dasgupta, A., Dasgupta, N. and Das, S.K., A micro-convection model for thermal conductivity of nanofluid, *Pramana-Journal of Physics*, 2005, 65 (5), 863-869.
- [15] Khanafer, K., Vafai, K. and Lightstone, M., Buoyancy-driven Heat Transfer Enhancement in a Two-dimensional Enclosure Utilizing Nanofluids, *Int. J. Heat and Mass Transfer*, 2003, 46 (19), 3639-3653.

- [16] Jou, R.Y. and Tzeng, S.C., Numerical research of nature convective heat transfer enhancement filled with nanofluids in rectangular enclosures, *International Communications in Heat and Mass Transfer*, 2006, 33 (6), 727–736.
- [17] Putra, N., Roetzel, W. and Das, S.K., Natural convection of nano-fluids, *Heat and Mass Transfer*, 2003, 39 (8-9), 775-784.
- [18] Wen, D. and Ding, Y., Natural Convective Heat Transfer of Suspensions of Titanium Dioxide Nanoparticles (Nanofluids), *IEEE Transactions on Nanotechnology*, 2006, 5 (May), 220-227
- [19] Nnanna, A.W.A., Experimental Model of Temperature-Driven Nanofluid, *ASME J. of Heat Transfer*, 2007, 129 (6), 697-704.
- [20] Kwak, K. and Kim, C., Viscosity and thermal conductivity of copper oxide nanofluid dispersed in ethylene glycol, *Korea-Australia Rheology Journal*, 2005, 17 (2), 35-40.
- [21] Chang, H, Jwo, C.S., Lo, C.H., Tsung, T.T., Kao, M.J. and Lin, H.M., Rheology of CuO nanoparticle suspension prepared by ASNSS, *Rev. Adv. Material Science*, 2005, 10, 128-132.
- [22] Ding, Y., Alias, H., Wen, D. and Williams, R.A., Heat transfer of aqueous suspensions of carbon nanotubes (CNT nanofluids), *Int. J. Heat and Mass Transfer*, 2006, 49 (1-2), 240-250.
- [23] Santra, A.K., Sen, S. and Chakraborty, N., Study of Heat Transfer Augmentation in a Differentially Heated Square Cavity using Copper–Water Nanofluid, *Int. J. Thermal Sciences*, 2008, 47 (9), 1113-1122.
- [24] Bird, R.B., Stewart, W.E. and Lightfoot, E.N., *Transport Phenomena*, John Wiley & Sons, Singapore, 1960.
- [25] Patankar, S.V, Numerical Heat Transfer and Fluid Flow, *Hemisphere*, Washington D. C., 1980.
- [26] de Vahl Davis, G., Natural Convection of Air in a Square Cavity, a Benchmark Numerical Solution, *Int. J. Numer. Methods Fluids*, 1962, 3, 249-264.